

Shell Stabilization of Super- and Hyperheavy Nuclei Without Magic Gaps

M. Bender,¹ W. Nazarewicz,²⁻⁴ P.-G. Reinhard^{5,6}

¹*Gesellschaft für Schwerionenforschung, Planckstrasse 1, D-64291 Darmstadt, Germany*

²*Department of Physics and Astronomy, University of Tennessee, Knoxville, Tennessee 37996*

³*Physics Division, Oak Ridge National Laboratory, P.O. Box 2008, Oak Ridge, Tennessee 37831*

⁴*Institute of Theoretical Physics, Warsaw University, ul. Hoża 69, PL-00681, Warsaw, Poland*

⁵*Institut für Theoretische Physik II, Universität Erlangen-Nürnberg, Staudtstrasse 7, D-91058 Erlangen, Germany*

⁶*Joint Institute for Heavy Ion Research, Oak Ridge National Laboratory, P. O. Box 2008, Oak Ridge, Tennessee 37831*

(March 23, 2001)

Quantum stabilization of superheavy elements is quantified in terms of the shell-correction energy. We compute the shell correction using self-consistent nuclear models: the non-relativistic Skyrme-Hartree-Fock approach and the relativistic mean-field model, for a number of parametrizations. All the forces applied predict a broad valley of shell stabilization around $Z = 120$ and $N = 172-184$. We also predict two broad regions of shell stabilization in hyperheavy elements with $N \approx 258$ and $N \approx 308$. Due to the large single-particle level density, shell corrections in the superheavy elements differ markedly from those in lighter nuclei. With increasing proton and neutron numbers, the regions of nuclei stabilized by shell effects become poorly localized in particle number, and the familiar pattern of shells separated by magic gaps is basically gone.

The synthesis of superheavy elements (SHE) has been in the focus of heavy-ion physics for more than three decades. The last few years have seen significant progress in our quest for reaching the region of long-lived SHE. Light isotopes of the elements $Z = 110-112$ have been safely established at GSI Darmstadt and JINR Dubna [1–3]. These isotopes are expected to be strongly deformed thanks to the (predicted) deformed shells $Z = 108$ and $N = 162$ (see Refs. [4–6] and references quoted therein). These new nuclides could be unambiguously identified by their characteristic α -decay chains leading to already known isotopes. Even heavier and more neutron-rich nuclides have been announced just recently by GSI (${}_{160}^{270}\text{110}$) [7]; Dubna (${}_{171}^{283}\text{112}$, ${}_{173-175}^{287-289}\text{114}$, and ${}_{176}^{292}\text{116}$) [8]; and Berkeley (${}_{175}^{293}\text{118}$) [9]. The α -decay chains of those nuclei cannot be linked to any known nuclides as they end with fissioning nuclei. However, these results yet need to be confirmed [3,10,11].

The mere existence of SHE relies on quantum mechanics. According to the classical liquid-drop picture, all superheavy nuclei should be unstable against spontaneous fission — due to the huge Coulomb repulsion. However, additional stabilization of binding energy is possible thanks to shell effects which generate local minima in the nuclear potential energy surface in the regions where the level density around the Fermi level is lowered. The detailed energy balance between the local minima is dictated by the distribution of spherical single-particle orbitals. In some cases the minima are sufficiently deep to stabilize the nucleus against spontaneous fission; the delay in the spontaneous fission half-lives due to the shell effects can be as much as 15 orders of magnitude for $Z \gtrsim 106$ [12].

The half-lives of the known isotopes of elements with $Z > 105$ are predominantly limited by α decay and decrease from 0.9 s for ${}_{157}^{263}\text{106}$ to 0.2 ms for ${}_{165}^{277}\text{112}$. These isotopes decay mostly by groups of successive α particles.

Although shell corrections strongly influence Q_α values, there is no simple correlation between the magnitude of shell effects and α -decay half-lives [13]. For instance, if the shell corrections are nearly constant in a broad region of particle numbers, this will have very little influence on Q_α values; hence on T_α .

The subject of the present paper is the shell stabilization quantified in terms of the shell correction E_{shell} . It is obtained from decomposing the self-consistent binding energy E_{tot} as

$$E_{\text{tot}} \approx \tilde{E} + E_{\text{shell}}, \quad (1)$$

where \tilde{E} is the average energy that changes smoothly with particle number. (In microscopic-macroscopic approaches, \tilde{E} is approximated by the liquid drop or droplet model energy.) The shell stabilization of SHE as predicted by macroscopic-microscopic models has already been extensively discussed in the literature [5,14,15]. It is the aim of the present study to analyze shell corrections in the superheavy region in the framework of self-consistent mean-field models. To this end, we apply the two most widely used approaches, namely the Skyrme-Hartree-Fock (SHF) theory and the relativistic mean-field (RMF) theory. (For a brief overview, see Ref. [16].) In the previous paper by Kruppa *et al.* [17], the shell energy extracted from self-consistent single-particle spectra along a few selected isotopic and isotonic chains was discussed. Here we present a large-scale survey of spherical shell energies throughout the whole landscape of conceivable SHE.

There is a world of different parametrizations for SHF as well as RMF. They agree more or less in their performance for stable nuclei but can yield differing predictions in extrapolations. For example, magic shell closures in SHE are at variance [13,17–19]. Interestingly, it has been concluded in Ref. [17] that both the SHF and RMF calculations were internally consistent. That is, all the Skyrme

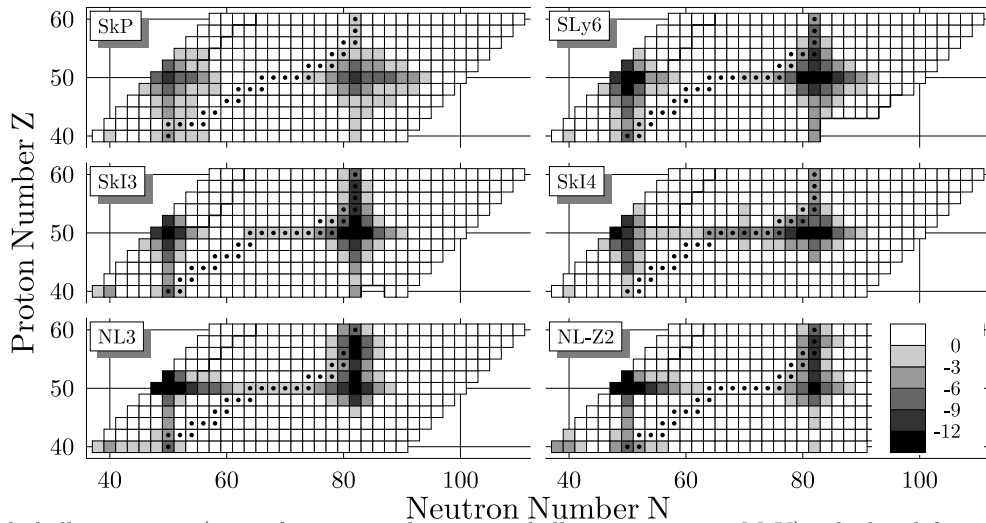


FIG. 1. Total shell correction (sum of proton and neutron shell corrections; in MeV) calculated for spherical even-even nuclei. The thick solid lines denote two-particle drip lines. Black squares mark nuclei calculated to be stable with respect to β decay. White color indicates nuclei with positive shell corrections, black color denotes nuclei with E_{shell} beyond -12 MeV.

models with conventional spin-orbit force predicted the strongest spherical shell effect at $N = 184$ and $Z = 124$, 126, while all the RMF forces clearly preferred $N = 172$ and $Z = 120$, and SHF parameterizations with relativistically extended spin-orbit interaction were in between.

In view of these differences, we consider several parametrizations per model. We use a selection of forces which have been found earlier to represent the whole range of possible predictions for spherical shell closures. For the RMF, we consider the parametrizations NL3 [20] and NL-Z2 [19]. Both represent recent fits which perform very well with respect to global ground-state properties but differ in detail. NL3 reproduces well isotopic trends, while NL-Z2 also fits the electromagnetic nuclear form factor. For the SHF, we consider SkP [21] as a representative for a force with effective nucleon mass $m^*/m = 1$, leading to a comparatively large density of single-particle levels. All other SHF forces employed here have smaller effective masses around $m^*/m \approx 0.7$. SLy6 [22] was adjusted with particular emphasis on isotopic trends and neutron matter. SkI3 and SkI4 [23] employ an extended form of the spin-orbit force which was found to be necessary for a description of isotope shifts in heavy Pb isotopes. For SkI3, the extension was restricted to map the spin-orbit structure of the RMF as closely as possible.

The shell energies are computed using the same prescription as outlined in Ref. [17]. This procedure, based on the Green's function approach to the level density, is better suited for the calculation of weakly bound systems than the traditional approach. This is important in the context of nuclei considered here since some of the predicted regions of shell stability lie very close to the proton drip line. In our calculations, we include a large space of single-particle states up to 50 MeV above the Fermi energy. Since most of these states are continuum (positive-energy) states, the contribution from a parti-

cle gas (treated in the same numerical box) has to be removed [17]. Pairing correlations are ignored.

The calculations are restricted to spherical symmetry. Consequently, the calculated shell corrections represents in most cases an upper bound. In many cases, deformation does provide an additional binding, i.e., pulls to even stronger shell stabilization. Unfortunately, large-scale symmetry-unconstrained calculations of shell effects in the SHE are currently beyond our reach. This is because triaxial [13] and reflection-asymmetric [24] shapes must be considered together with more exotic topologies (e.g., bubble [25], toroidal, and rod structures) which might become favored for the heaviest systems investigated here.

For nuclei up to $Z = 82$, E_{shell} is always sharply peaked at shell closures [26,27]. Figure 1 shows an example from the Sn region. The magic numbers $Z = 50$, $N = 50$, and $N = 82$ clearly stick out for all forces. One basically sees sharp stripes along magic proton and neutron numbers. All forces show the same magic numbers, but there are some differences in detail. The overall strength of the shell effect seems to scale with effective mass, with SkP giving the smallest shell energies, while they are most pronounced for NL3.

The systematics of shell corrections change dramatically when going to SHE; see Fig. 2. Instead of narrow stripes of large E_{shell} localized around magic numbers, all forces employed predict a wide area of shell stabilization which spreads over all shell closures predicted by the various forces. Unlike in normal nuclei, large shell corrections in SHE can appear slightly away from shell closures. This was, in fact, already recognized in macroscopic-microscopic models [5,14,15]. As a consequence, the significant differences seen in the prediction of magic shells through various binding-energy indicators (such as δ_{2q} [18]) are much mellowed by the generally softer pattern of the shell energy. We will discuss that aspect in more

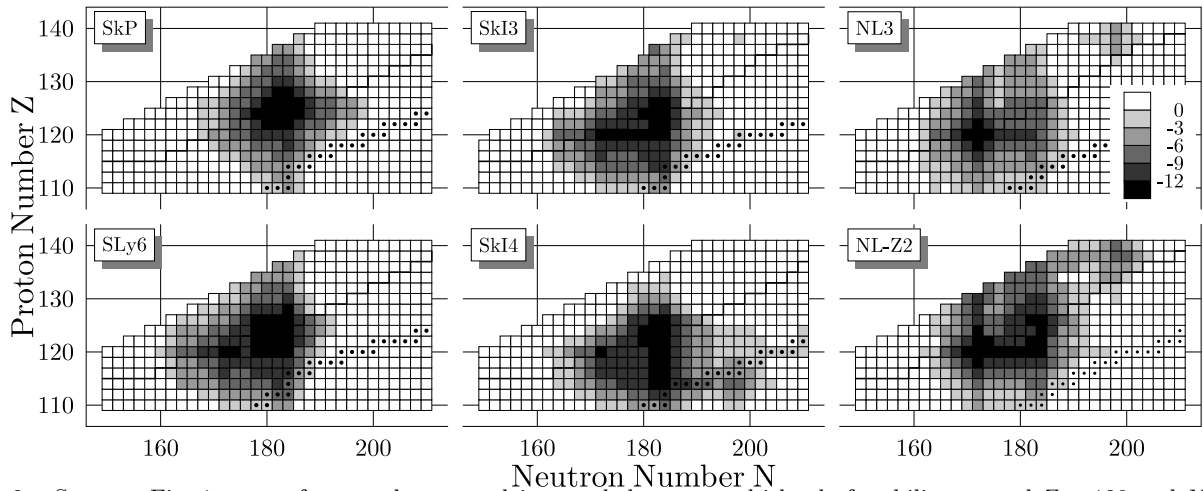


FIG. 2. Same as Fig. 1 except for superheavy nuclei around the expected island of stability around $Z = 120$ and $N = 180$. The scale for E_{shell} is the same as in Fig. 1. See Ref. [17] for the individual shell correction of protons and neutrons along cuts through these maps.

detail below. One of the common features seen in Fig. 2 is that the region of nuclei with largest shell corrections forms a triangle with the base at $N = 184$ and the outer corner at ${}_{172}^{292}120$. This happens because the existence of the $N = 172$ neutron subshell is strongly coupled to the proton subshell closure at $Z = 120$ [19].

At second glance, however, one also sees differences among various parameterizations. More stable nuclei are found above $Z = 120$ for SkP which predicts the proton gap at $Z = 126$, while the center of gravity is clearly shifted below $Z = 120$ for SkI4 with its strong $Z = 114$ shell effect. The other forces reside in between. A somewhat different bias is also seen for the extension in neutron direction. SkP predict strong shell effects for a number of nuclei with $N > 184$, while other forces fill basically the landscape between the two magic numbers $N = 172$ and $N = 184$. There are also some differences concerning the overall area of the stabilized region. For instance, NL3 makes it much smaller than all other forces. Of course, for a quantitative discussion, one needs to account for deformation effects which will serve to extend the island of shell stabilization. For example, the well-known region of deformed shell-stabilized SHE located around ${}_{162}^{270}\text{Hs}_{108}$ [4–6] is missing in Fig. 2, as well as the deformed shell closure at $N = 174$ [28,29].

Figure 3 takes a daring glance to even heavier nuclei with $Z > 126$ (hyperheavy elements). There are several broad valleys of spherical shell stability showing up that extend around the actual shell closures. This is a common feature of very heavy nuclear systems. Differences between the forces, however, grow dramatically in the hyperheavy region. The upper limit for the plots is chosen to stay below the region where the novel topologies, i.e., semi-bubbles and bubbles, are believed to coexist [25]. As the RMF predicts the lower border of this transitional region at smaller values of Z than SHE, we set different upper limits of the displayed area in both approaches. By

inspecting Fig. 3 carefully, one can see rather large differences in E_{shell} predicted in different calculations. That is no surprise because fine details of shell structure play an increasing role with increasing nuclear size. Nevertheless, there still remains an overall agreement concerning the position of the regions of stability, around $N = 258$ and around $N = 308$. The RMF parameterizations are more pessimistically predicting only faint effects, while SHF produces a strong stabilization at $N = 308$.

It is an open question whether for these hyperheavy elements the actual shell corrections are sufficient to prevent (or significantly slow down) spontaneous fission. One would expect that, with increasing Z , the Coulomb force would act increasingly against stability. In particular, the role of triaxial or reflection asymmetric degrees of freedom must be considered when assessing the stability of hyperheavy nuclei to fission.

Figure 4 shows the single-particle spectra for three typical nuclei from the three regions of large shell correction discussed in this paper. For ${}^{132}\text{Sn}$, proton and neutron magic gaps appear in all models. The patterns of single-particle levels are significantly different for the two regions of SHE. Firstly, with increased mass, the overall level density grows as $\propto A^{1/3}$. Secondly, no pronounced and uniquely preferred energy gaps appear in the spectrum. This shows that shell closures which are to be associated with the gaps in the spectrum are not robust in that region. Tiny changes in, e.g., spin-orbit properties can shift the gaps substantially; see [13,19] for a thorough discussion. Protons are more sensitive in that respect than neutrons.

Interestingly, similar problems are encountered in atomic calculations of the electron shell structure of SHE [30]. Due to the large density of valence electron shells, it is extremely difficult to make robust predictions of chemical properties of SHE.

A close inspection of Fig. 4 allows for a rather good

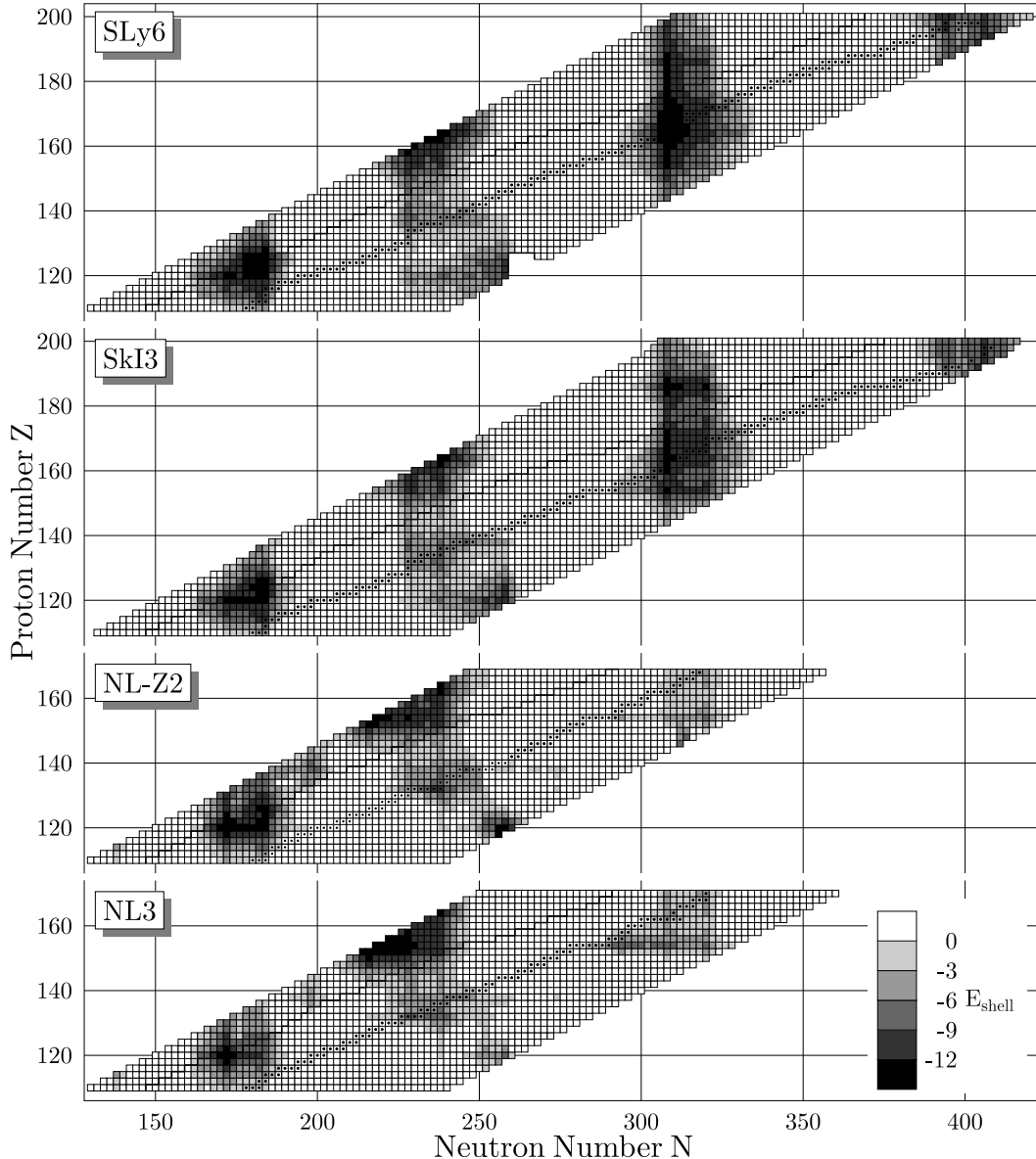


FIG. 3. Same as in Figs. 1 and 2 but for larger neutron and proton numbers (up to $Z = 200$ for SHF and $Z = 170$ for RMF) calculated with the subset of forces as indicated. The energy scale is kept the same as in the other figures.

understanding of the shell-correction pattern discussed above. For instance, in ${}_{184}^{310}126$ there appear low- j single-particle orbitals at the Fermi surface ($3p_{1/2}$ and $3p_{3/2}$ in the protons between $Z = 120$ and 126 and $4s_{1/2}$, $3d_{3/2}$, and $3d_{5/2}$ in the neutrons between $N = 172$ and 184). The low $(2j+1)$ degeneracy of these shells gives rise to reduced single-particle level densities; hence to a large negative shell-correction energy for a whole range of neighboring nuclei.

For hyperheavy nuclei, the level density is even higher, and no strong shell closures are predicted in most models. It is only in SLy6 and SkI3 that a relative large $N = 308$ gap is predicted, bounded by high- j shells. This is consistent with Fig. 3 which shows a rather strong neutron shell effect at $N = 308$ for these two forces.

In summary, we have investigated the spherical shell-stability of superheavy elements using state-of-the-art self-consistent models. The investigation of the systematics of shell energy reveals a new feature when going to very heavy systems. Beyond $Z = 82$ and $N = 126$, the familiar localization of the shell effect at magic numbers is basically gone. Instead, the theory predicts fairly wide areas of large shell stabilization. Consequently, there is a good chance to reach shell-stabilized SHE experimentally using a range of beam-target combinations.

The disappearance of a familiar pattern of magic numbers and the appearance of broad valleys of shell stability is due to (i) the rather large single-particle level density, and (ii) the appearance of many low- j shells around the Fermi level. This explains the robustness of the shell cor-

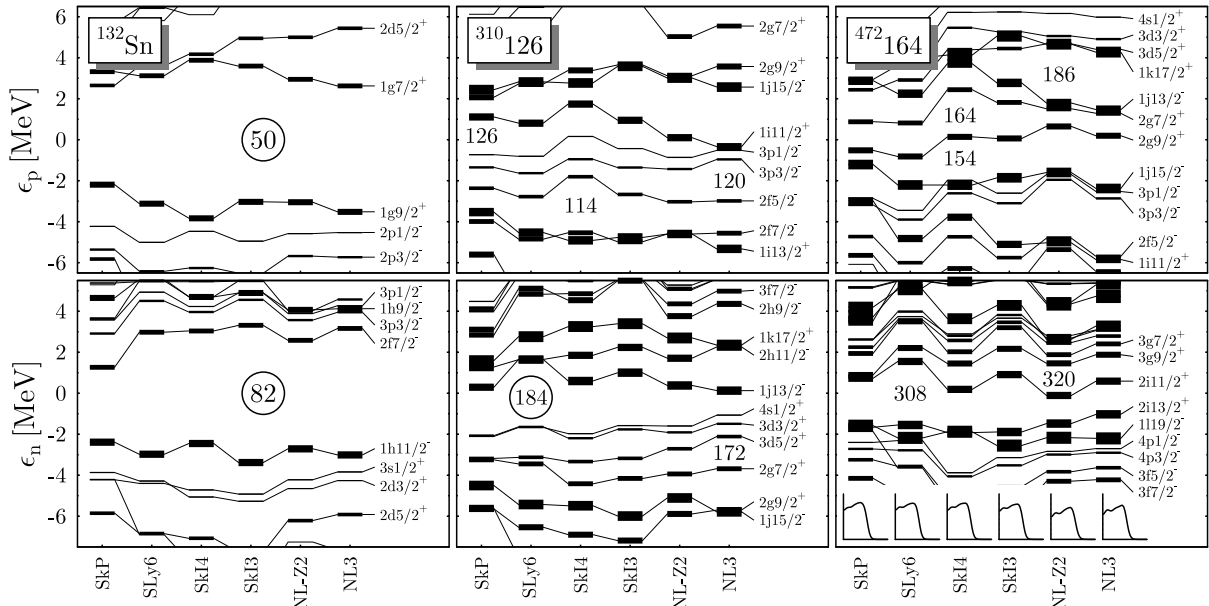


FIG. 4. Single-particle spectra of protons (top) and neutrons (bottom) for ^{132}Sn , $^{310}_{184}126$ and $^{472}_{308}164$. The single-particle energies are taken relative to the Fermi energy predicted by SLy6. The line thickness of each level is proportional to the $2j + 1$ degeneracy of the state. The inset in the rightmost panel shows the predicted radial neutron distributions. No bubble structure is predicted for $^{472}_{308}164$.

rection in a rather large range of SHE and at the same time the volatility of magic shell closures.

The results presented here have to be taken with a grain of salt. Large shell correction is a necessary, but not sufficient, condition for the appearance of long-lived SHE. The calculations presented in this paper serve as a starting point for subsequent studies of deformed shell effects and fission barriers in superheavy and hyperheavy nuclei.

ACKNOWLEDGMENTS

This work was supported in part by Bundesministerium für Bildung und Forschung (BMBF), Project No. 06 ER 808; by Gesellschaft für Schwerionenforschung (GSI); and by the U.S. Department of Energy under Contract Nos. DE-FG02-96ER40963 (University of Tennessee), DE-FG05-87ER40361 (Joint Institute for Heavy Ion Research), and DE-AC05-00OR22725 with UT-Battelle, LLC (Oak Ridge National Laboratory).

[1] S. Hofmann, Rep. Prog. Phys. **61**, 639 (1998).
[2] S. Hofmann and G. Müntzenberg, Rev. Mod. Phys. **72**, 733 (2000).
[3] P. Armbruster, Ann. Rev. Nucl. Part. Sci. **50**, 411 (2000).
[4] S. Ćwiok, V. V. Pashkevich, J. Dudek, and W. Nazarewicz, Nucl. Phys. **A410**, 254 (1983).

[5] P. Möller and J. R. Nix, J. Phys. **G 20**, 1681, (1994).
[6] R. Smolańczuk, J. Skalski, and A. Sobczewski, Phys. Rev. C **52**, 1871 (1995).
[7] S. Hofmann *et al.*, Eur. Phys. J. A **10**, 5 (2001).
[8] Yu. Ts. Oganessian *et al.*, Eur. Phys. J. A **5**, 68 (1999); Phys. Rev. Lett. **83**, 3154 (1999); Nature **400**, 209 (1999); Phys. Rev. C **62**, 041604(R) (2000); Phys. Rev. C **63**, 011301(R) (2001).
[9] V. Ninov *et al.*, Phys. Rev. Lett. **83**, 1104 (1999).
[10] P. Armbruster, Eur. Phys. J. **A7**, 23 (2000).
[11] K.-H. Schmidt, Eur. Phys. J. **A8**, 141 (2000).
[12] G. Müntzenberg, Rep. Prog. Phys. **51**, 57 (1988).
[13] S. Ćwiok, J. Dobaczewski, P.-H. Heenen, P. Magierski, and W. Nazarewicz, Nucl. Phys. **A611**, 211 (1996).
[14] P. Möller and J. R. Nix, Nucl. Phys. **A549**, 84 (1992).
[15] R. Smolańczuk, Phys. Rev. C **56**, 812 (1997).
[16] P.-G. Reinhard, M. Bender, and J. A. Maruhn, Comments on Nuclear and Particle Physics, in print.
[17] A. T. Kruppa, M. Bender, W. Nazarewicz, P.-G. Reinhard, T. Vertse, and S. Ćwiok, Phys. Rev. C **61**, 034313 (2000).
[18] K. Rutz, M. Bender, T. Bürvenich, T. Schilling, P.-G. Reinhard, J. A. Maruhn, and W. Greiner, Phys. Rev. C **56**, 238 (1997).
[19] M. Bender, K. Rutz, P.-G. Reinhard, J. A. Maruhn, and W. Greiner, Phys. Rev. C **60**, 034304 (1999).
[20] G. A. Lalazissis, J. König, and P. Ring, Phys. Rev. C **55**, 540 (1997).
[21] J. Dobaczewski, H. Flocard, and J. Treiner, Nucl. Phys. **A422**, 103 (1984).
[22] E. Chabanat, P. Bonche, P. Haensel, J. Meyer, and R. Schaeffer, Nucl. Phys. **A635**, 231 (1998); Nucl. Phys. **A643**, 441(E) (1998).
[23] P.-G. Reinhard and H. Flocard, Nucl. Phys. **A584**, 467

- (1995).
- [24] M. Bender, K. Rutz, P.-G. Reinhard, J. A. Maruhn, and W. Greiner, *Phys. Rev. C* **58**, 2126 (1998).
 - [25] J. Dechargé, J.-F. Berger, K. Dietrich, and M. S. Weiss, *Phys. Lett.* **B451**, 275 (1999).
 - [26] I. Ragnarsson and R. K. Sheline, *Phys. Scr.* **29**, 385 (1984).
 - [27] S. G. Nilsson and I. Ragnarsson, *Shapes and Shells in Nuclear Structure* Cambridge University Press, Cambridge 1995.
 - [28] S. Ćwiok, P.-H. Heenen, and W. Nazarewicz, *Phys. Rev. Lett.* **83**, 1108 (1999).
 - [29] M. Bender, *Phys. Rev. C* **61**, 031302(R) (2000).
 - [30] P. Schwerdtfeger and M. Seth, *Relativistic Effects of the Superheavy Elements*, Encyclopedia of Computational Chemistry, Vol. 4, Wiley, New York, 1998, p. 2480.